

Computer-simulation study of the thermal conductivity of amorphous insulating solids

Vladislav Malyskin* and Arthur R. McGurn

Department of Physics, Western Michigan University, Kalamazoo, Michigan 49008

(Received 15 December 1995; revised manuscript received 18 March 1996)

We study by computer simulation an amorphous solid modeled as a percolating cluster of atoms on the fcc lattice. The atoms interact by nearest neighbor Lennard-Jones pair potentials. In contrast to past simulation efforts, the present simulation allows for full three-dimensional motion of the atoms, and exhibits results for the thermal conductivity and density of states of the vibrational modes which differ from previous simulation results. [S0163-1829(96)02029-2]

Though there is a great difference between the temperature dependence and magnitude of the thermal conductivity of crystalline and amorphous insulating solids,¹⁻⁷ the thermal conductivities of amorphous insulating solids are found quantitatively as well as qualitatively to be very similar to one another. In general, three regions of temperature behavior are observed in amorphous insulating solids. These are (1) for $T \leq 1$ K the thermal conductivity exhibits a T^β power law behavior with $1 \leq \beta \leq 2$, (2) for $1 \leq T \leq 10$ K a plateau region is observed in which the thermal conductivity is relatively independent of temperature, (3) for $10 \leq T \leq 100$ K the thermal conductivity again exhibits a monotonic increase with increasing T .¹⁻⁷ As these three features are present in most amorphous insulating solids, exhibiting the same orders of magnitude of the thermal conductivity, a comprehensive theoretical treatment of the thermal conductivity must exhibit these properties for quite general amorphous geometries and atomic interactions.

Recently, computer-simulation work on vibrational excitations and the thermal conductivity of amorphous insulating materials has been done by Sheng and Zhou.⁷ They considered a *scalar wave* treatment (atoms of the system only move in one dimension) of a system of atoms on an infinite percolating cluster (model of amorphous material) defined on a simple cubic lattice.

In this paper we shall present simulation results for the thermal conductivity of a percolating cluster (amorphous material) on which the atoms of the cluster are allowed fully three-dimensional (vector) vibrational displacements. Specifically, atoms in our model are taken to be on an infinite percolating cluster of a fcc lattice and to interact by nearest neighbor Lennard-Jones pair potentials. The choice of nearest neighbor pair potentials in our amorphous structures, however, precludes a treatment based on the simple cubic lattice as the simple cubic lattice with nearest neighbor pair potential interactions is mechanically unstable.

Our calculations for the thermal conductivity $K(T)$ are based on the relation

$$K(T) = \int_0^\infty \nu(\omega) C(\omega) D(\omega) d\omega, \quad (1)$$

where $\nu(\omega)$ is the phonon density of states in frequency,

$$C(\omega) = k_B \left(\frac{\hbar \omega}{k_B T} \right)^2 \frac{\exp[(\hbar \omega)/(k_B T)]}{\{\exp[(\hbar \omega)/(k_B T)] - 1\}^2}$$

is the specific heat at temperature T of a vibrational mode of frequency ω , and $D(\omega)$ is the diffusion constant of a phonon of frequency ω . Equation (1) does not make a distinction between the diffusivity of different types of modes of frequency ω , but rather treats all excitations of frequency ω the same.

The Hamiltonian of the system we study is $\mathcal{H} = \sum_i \mathbf{p}_i^2 / 2m + (1/2) \sum_i \sum_{\delta} u(|\mathbf{r}_{i+\delta} - \mathbf{r}_i|)$, i runs over the atoms, δ is such that $i + \delta$ sums over the nearest neighbors of the i th atom, and $u(r) = 4\epsilon[(\sigma/r)^{12} - (\sigma/r)^6]$ is the (12-6) Lennard-Jones pair potential with the fcc lattice constant $a_0 = 2^{1/6}\sigma$. From this system we remove at random a fraction $1 - p$ of the atoms. We then further remove all atoms in finite clusters, retaining only the atoms bound in the infinite percolating cluster.

The computation of $\nu(\omega)$ is based on the harmonic approximation using recursive methods.⁸ The computation of $D(\omega)$ is based on the full anharmonic Hamiltonian.

Our density of states calculations rely on recursion methods found in the work by Haydock *et al.*⁸ and Nex.⁹ For our random network, $\nu(\omega)$ [where $\nu(\omega)d\omega = n(\omega^2)d\omega^2$ and $n(\omega^2)$ is the density of modes in ω^2], can be written in terms of a summation over the local density of states $n_{i,\alpha}(\omega^2)$ at each atomic site i for the component of atomic motion along the α axis, e.g., $n(\omega^2) = \sum_{i,\alpha} n_{i,\alpha}(\omega^2)$ where $\int n_{i,\alpha}(\omega^2) d\omega^2 = 1$. In terms of the dynamical matrix \mathcal{D} of the vibrational system

$$\begin{aligned} n_{i,\alpha}(\omega^2) &= -\frac{1}{\pi} \text{Im} G_{i,i}^{\alpha,\alpha}(\omega^2) \\ &= -\frac{1}{\pi} \langle i, \alpha | (\omega^2 + i0 - \mathcal{D})^{-1} | i, \alpha \rangle \end{aligned} \quad (2)$$

and $|i, \alpha\rangle$ is a normalized state of motion of the i th atom along the α axis.

Expressing the dynamical matrix \mathcal{D} in tridiagonal form

$$\mathcal{D}_{mn}^{TD} = \begin{cases} a_m^{i,\alpha}, & n = m, \\ b_{m+1}^{i,\alpha}, & n = m + 1, \\ b_m^{i,\alpha*}, & n = m - 1, \\ 0, & \text{otherwise,} \end{cases} \quad (3)$$

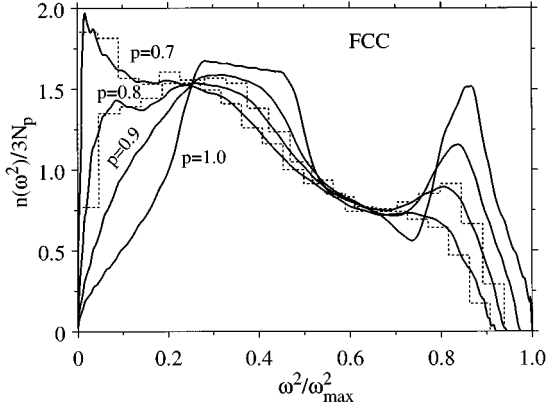


FIG. 1. The density of states $n(\omega^2)$ vs ω^2 for a system, composed of N_p atoms (atoms on the percolating cluster) for $p=0.7$, $p=0.8$, $p=0.9$, and $p=1.0$. In this plot ω_{\max} is the maximal vibrational frequency of the $p=1.0$ fcc system. Results for $p=0.7$ and $p=0.8$ obtained by directly counting the eigenvalues of the dynamical matrix computed for a reduced array of 864 sites (dashed line histogram results) are also shown.

$G_{i,i}^{\alpha,\alpha}(\omega^2)$ can be expanded as a continued fraction,

$$G_{i,i}^{\alpha,\alpha}(\omega^2) = \frac{1}{\omega^2 - a_1^{i,\alpha} - |b_2^{i,\alpha}|^2 \frac{1}{\omega^2 - a_2^{i,\alpha} - \dots}}, \quad (4)$$

where $\{a_n^{i,\alpha}, b_n^{i,\alpha}\}$ can be calculated using methods similar to those in Ref. 8. In general, we use 20–40 sets of $\{a_n^{i,\alpha}, b_n^{i,\alpha}\}$ for a given $|i,\alpha\rangle$. The termination used (see Ref. 10 for details) is based on the development of an expression for $n_{i,\alpha}(\omega^2)$ from its continued fraction representation and the derivative of $\int \omega^2 n_{i,\alpha} d\omega^2$ with respect to ω^2 .^{9,11}

We have considered a cube of fcc lattice of $21 \times 21 \times 21$ conventional unit cells with periodic boundary conditions. We have determined $n(\omega^2)$ using 1000 and 6000 different $|i,\alpha\rangle$. Little difference was found between $n(\omega^2)$ computed using 1000 and using 6000. In Fig. 1 we present results for $n(\omega^2)$ versus ω^2 for $p=1$, agreeing with Ref. 12. In Fig. 1 results are shown for $p=0.9$, $p=0.8$, and $p=0.7$. Some of these results are compared to results obtained by the counting of eigenvalues of the dynamical matrix for an array of 864 sites.

The phonon diffusion coefficient $D(\omega)$ (proportional to the total mean free path for phonon scattering in the system^{6,7}) is given by $1/D(\omega) = 1/D_N(\omega) + 1/D_{\text{TL}}(\omega)$ where $D_N(\omega)$ is for processes involving scattering from a fixed network and $D_{\text{TL}}(\omega)$ is for processes involving scattering accompanying a change in network geometry between metastable states. The processes contributing to $D_{\text{TL}}(\omega)$ are treated in the context of the two-level state theory^{2,3} which uses

$$\frac{1}{l_{\text{TL}}(\omega)} = A \frac{\hbar \omega}{k_B} \tanh\left(\frac{\hbar \omega}{2k_B T}\right) + \frac{A}{2} \frac{1}{k_B / \hbar \omega + 1/B T^3} \quad (5)$$

for fitting parameters A and B to give the low temperature behavior of $l_{\text{TL}}(\omega) = (3/\bar{v})D_{\text{TL}}(\omega)$ where \bar{v} is the average phonon velocity [Eq. (5) was taken from the Ref. 6 and differs from that used by Sheng and Zhou,⁷ see Ref. 11].

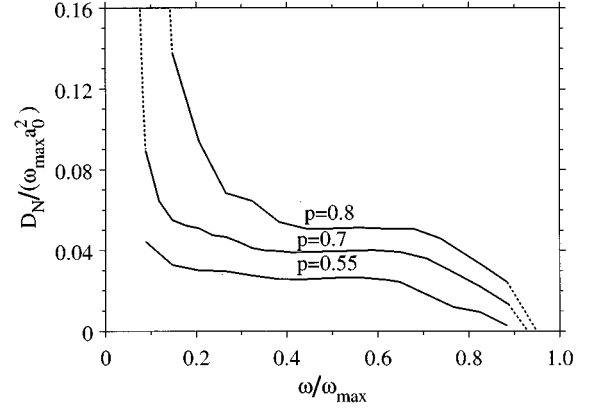


FIG. 2. The diffusion coefficient $D_N(\omega)$ vs ω for $p=0.55$, $p=0.7$, and $p=0.8$. In this plot ω_{\max} is the maximal vibrational frequency of the $p=1.0$ fcc system and a_0 is the nearest neighbor separation (lattice constant) on the fcc lattice.

In computing $D_N(\omega)$ we study the system dynamics when, to a single atom at the center of the percolating cluster, we apply a time-dependent force of the form

$$\mathbf{F}(t) = \begin{cases} \mathbf{F}_0 \sin(\omega t) \exp[-(\gamma \omega t)^2], & -t_0 \leq t \leq t_0, \\ 0, & \text{otherwise,} \end{cases} \quad (6)$$

where $|\gamma \omega t_0|^2 \geq 3.8$. The simulation begins at $t = -t_0$. The amplitude distribution of the driving force as a function of frequency in our calculations has a half width at half maximum of $\Delta \omega \approx 0.07 \omega$.

The diffusion coefficient, $D_N(\omega)$, is computed¹¹ by studying the time dependence of $\langle R^2 \rangle = \sum_i u_i \mathcal{R}_i^2 / \sum_i u_i$, where \mathcal{R}_i is the equilibrium position vector of the i th atom measured relative to the equilibrium position of the atom driven by the force defined in Eq. (6) and $u_i = \mathbf{p}_i^2 / 2m + (1/2) \sum_{\delta} \mu(|\mathbf{r}_{i+\delta} - \mathbf{r}_i|)$. (We have taken a different form for u_i than that used by Sheng and Zhou,⁷ see Refs. 11 and 13.)

In Fig. 2 are results for the diffusion coefficient, $D_N(\omega)$ for $p=0.55$, $p=0.7$, and $p=0.8$. The solid lines in this figure represent $D_N(\omega)$ computed as described above but the dashed lines represent an interpolation which we discuss below. These results were obtained for percolating clusters created from an fcc region of $37 \times 37 \times 37$ conventional unit cells with periodic boundary conditions.

It is well known that at low frequencies $D_N(\omega)$ is dominated by Rayleigh scattering¹⁴ [$D_N(\omega) \xrightarrow{\omega \rightarrow 0} C_d \omega^{-4}$]. This fact can be used to estimate the low frequency behavior of $D_N(\omega)$. Specifically, in Fig. 2 at low frequency we have approximated $D_N(\omega) = C_d \omega^{-4}$ (dotted lines) where C_d is chosen to match the simulation results for $D_N(\omega)$ (solid lines) at their lowest frequency.

At the upper frequency limit of $D_N(\omega)$, we use an interpolation scheme to set $D_N(\omega)$ to zero at the upper frequency band edge (see Ref. 15). In this case we use a linear interpolation from the upper edge of the simulation computed $D_N(\omega)$ (solid lines) to zero at $\omega = 0.96 \omega_{\max}$ for $p=0.7$ and $\omega = 0.97 \omega_{\max}$ for $p=0.8$, where ω_{\max} is the upper band edge of the $p=1.0$ system.

For the thermal conductivity we use $\nu(\omega)$, $D(\omega)$, and the specific heat in Eq. (1) to obtain results as a function of T .

TABLE I. Parameters used for the thermal conductivity calculation. ρ (g/cm^3), \bar{v} ($10^5 \text{ cm}/\text{sec}$), Θ_D (K), A ($\text{cm}^{-1} \text{ K}^{-1}$), B (10^{-3} K^{-2}), m_{unit} ($1.66054 \times 10^{-24} \text{ g}$), n_{unit} , and a_1 (\AA).

Material	ρ	\bar{v}	Θ_D	A	B	m_{unit}	n_{unit}	a_1
<i>a</i> -SiO ₂	2.2	4.1	300	360	3.0	60.08	3	2.78
<i>a</i> -Se	4.3	1.19	113	880	20.0	78.96	1	3.51
<i>PMMA</i>	1.2	1.79	150	1000	0.3	100.12	15	2.36

The resulting integral for the thermal conductivity depends on the fcc lattice constant a_0 , ω_{max} , \bar{v} , A and B . Values for \bar{v} , A , and B are listed in Table I of Ref. 6, and we have taken these over directly in obtaining the result for $K(T)$. To obtain ω_{max} we have made the approximation $\hbar \omega_{\text{max}} = k_B \Theta_D$, where Θ_D is the Debye temperature listed in Table I of Ref. 6. A value of the lattice constant a_0 can be obtained¹¹ from $a_0 = a_1 p^{1/3}$, p is the atomic concentration, $a_1 = (\sqrt{2} m_{\text{unit}} / \rho n_{\text{unit}})^{1/3}$ and ρ is the mass density (taken from Table I of Ref. 6), m_{unit} is the mass of the molecular unit which is repeated on the amorphous network, and n_{unit} is the number of atoms in the molecular unit. The a_0 is chosen so that the number of vibrational modes per volume is the same in our model as in the experimental material we compare with. In Table I we present parameters we extracted as above for *a*-Se, *a*-SiO₂, and *PMMA*.

In Fig. 3 we present $K(T)$ versus T computed for $p=0.7$ and $p=0.8$, respectively. Qualitative agreement is found between the thermal conductivities in Fig. 3 and the

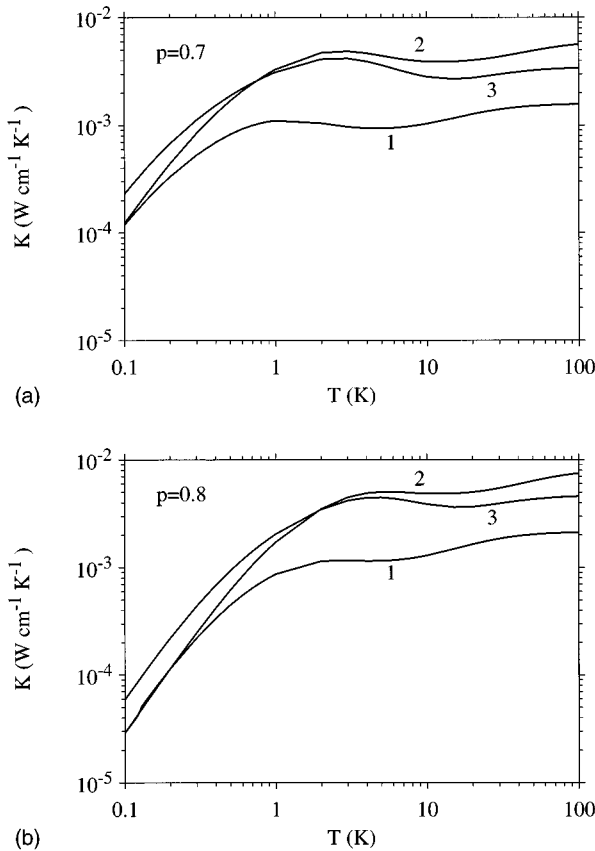


FIG. 3. The thermal conductivity vs temperature for parameters for *a*-Se (1), *a*-SiO₂ (2), and *PMMA* (3), in Table I.

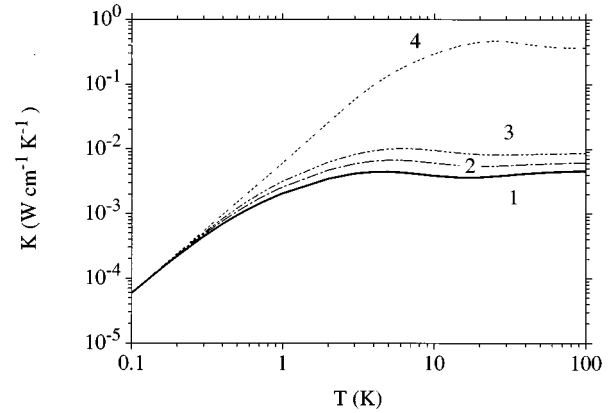


FIG. 4. Thermal conductivity, calculated for Table I *PMMA* parameters, $p=0.8$, C_d (1), $2C_d$ (2), $4C_d$ (3), and $C_d \rightarrow \infty$ (4).

experimental data for these materials presented in Fig. 2 of Ref. 6. We do not expect nor do we find quantitative agreement between our Fig. 3 results and the results in Fig. 2 of Ref. 6. This is due to the fact that our model does not reflect the structure of *a*-Se, *a*-SiO₂, and *PMMA*. (Sheng and Zhou in their Fig. 4 choose parameters to force a fit between theory and experiment. We have not done this.)

At $T \leq 1$ K in which the diffusivity is dominated by two level scattering, we find $K(T) \propto T^\beta$, where at low frequencies $\nu(\omega) \propto \omega^\beta$. Our results for $p=0.8$ exhibit Debye behavior for $\omega/\omega_{\text{max}} \leq 0.2$ and give $\beta=2$ but our $p=0.7$ results, which only exhibit Debye behavior for $\omega/\omega_{\text{max}} \leq 0.05$, give $1 < \beta < 2$. These types of power law behaviors compare favorably with experiment. The scalar wave results of Sheng and Zhou, however, are based on models which exhibit only $\beta=2$ Debye like behavior.^{11,14,16}

The $C_d \omega^{-4}$ contribution to $D_N(\omega)$ from Rayleigh scattering is important in determining the low temperature limit of the plateau region. This can be seen from Fig. 4. Results are shown for C_d , $2C_d$, $4C_d$, and $C_d \rightarrow \infty$ where C_d is the Rayleigh scattering fitting coefficient used in Fig. 3 for *PMMA* and $p=0.8$. In general, for C_d , $2C_d$, $4C_d$ the character of the thermal conductivity is little changed from the $C_d \omega^{-4}$ fit. In the extreme limit that Rayleigh scattering is ignored, a small plateau region is observed even though the thermal conductivity determined in this case is too large. In this last limit the plateau region is also observed to begin at too large a value of T . For $T \geq 10$ K, all curves for $K(T)$ eventually increase monotonically with increasing T . This behavior follows primarily from the specific heat.

To conclude we find upon comparison with the scalar wave theory the following.

(1) Both models exhibit diffusion coefficients which decrease in magnitude with decreasing atomic concentration p . The Rayleigh scattering dominates $D_N(\omega)$ at lower frequencies as p is decreased. At lowest frequencies the total diffusivity is determined by two level states scattering. As the frequency is increased a region is observed in which the total diffusivity is dominated by Rayleigh scattering and at the largest frequencies general scattering from the amorphous network is dominant.

(2) The vector treatment exhibits a density of states which differs considerably from the scalar wave model and accounts for the larger thermal conductivity values observed in our vector treatment. Our results, unlike the Sheng and Zhou results, exhibit a density of states which can depart (except for a very small neighborhood of $\omega=0$) from a quadratic variation with ω at very low frequencies.¹¹

(3) Both models exhibit the three regions of different temperature dependent behavior observed for $T \leq 100$ K. In both

models the plateau region and its lower temperature limit are determined by the Rayleigh scattering from the amorphous network. The exponent β in our model offers $1 \leq \beta \leq 2$ which is more realistic than $\beta=2$ observed in the scalar wave treatment.

This work was supported in part by National Science Foundation Grant No. DMR 92-13793. The authors would like to thank Professor Roger Haydock for supplying some of the recursive codes which were used in this work.

*On leave from: A. F. Ioffe Physical Technical Institute, 194021, St. Petersburg, Russia. Electronic address: malyshkin@ton.ioffe.rssi.ru

¹R.C. Zeller and R.O. Pohl, Phys. Rev. B **4**, 2029, (1971).

²P.W. Anderson, B.I. Halperin, and C.M. Varma, Philos. Mag. **25**, 1, (1972).

³W.A. Philips, J. Low Temp. Phys. **7**, 351 (1971)

⁴R. Berman, *Thermal Conduction in Solid* (Clarendon Press, Oxford, 1975).

⁵*Amorphous Solids: Low Temperature Properties*, edited by W.A. Philips (Springer-Verlag, Berlin, 1981).

⁶J.E. Graebner, B. Golding, and L.C. Allen, Phys. Rev. B **34**, 5696 (1986).

⁷P. Sheng and M. Zhou, Science, **253**, 539 (1991).

⁸R. Haydock, V. Heine, and M.J. Kelly, J. Phys. C **8**, 2591 (1975).

⁹C.M.M. Nex, Comput. Phys. Commun. **34**, 101 (1984).

¹⁰In our termination scheme we have replaced Eq. (3.8c) in Ref. 9 by $\partial w_i / \partial a_{n-1} = [\{q'_{n-1} p_{n-1} - p'_n q_{n-2} + w_i (p'_{n-1} p'_n - p''_n p_{n-1})\} / p_n'^2]_{E=E_i}$. This termination was used in routines we received from Professor Haydock. At the very lowest frequencies (i.e., $\omega/\omega_{\max} \leq 0.025$, where ω_{\max} is the maximum frequency in the pure fcc system, $n(\omega)$ fails to go to zero at

$\omega=0$ but begins to exhibit a bending which would eventually take it into the negative frequency region. To correct for this we have fitted out data for $n(\omega)$ below $\omega/\omega_{\max} \approx 0.025$ with a Debye form to give the correct $\omega \rightarrow 0$ limiting behavior.

¹¹V. Malyshkin (unpublished).

¹²J.C. Wheeler and M.G. Prais, Phys. Rev. B **10**, 2429 (1974).

¹³The choice of u_i in the text is a logical choice of a physical quantity to use in the computation of $\langle R^2 \rangle$ and $D_N(\omega)$. It is not the only choice and, for example, various linear combinations of $\mathbf{p}_i^2/2m$ and $(1/2)\sum_{\delta} \mu(|\mathbf{r}_{i+\delta} - \mathbf{r}_i|)$ can be used to evaluate $\langle R^2 \rangle$. We have found that our u_i avoids short period oscillatory behavior in $\langle R^2 \rangle$. The $D_N(\omega)$ computed from our u_i or its other various forms upon time averaging do not differ substantially from one another (see Ref. 15).

¹⁴D.P. Jones, N. Thomas, and W.A. Philips, Philos. Mag. B **38**, 271 (1978).

¹⁵S. John, in *Scattering and Localization of Classical Waves in Random Media*, edited by P. Sheng (Word Scientific, Singapore, 1990), p. 1.

¹⁶J.S. Lannin, H.F. Eno, and F.L. Luo, Solid State Commun. **25**, 81 (1977).